.

CHAPTER 1

Introduction

The utilization of contemporary technologies has become an obvious part of modern era. The versatile applications of these technologies make life easier and convenient. Among them, magnetism is one of the most exploited terms in contemporary technologies. The technology changes from simple compass to electrical generator, to computers, also from cassettes and video tapes to pen-drive, hard disk, magnetism truly changes the world. Moreover, the discovery of new novel magnetic materials enhances our knowledge, provide the new sight to see the world and enrich the technology.

1.1 Magnetism :: Introduction:

Magnetic materials contain ions which possess magnetic moment. Generally, total angular momentum consists of both spin and orbital angular momentum. Periodic motion of electron around nucleus generates the orbital angular momentum, whereas, spin angular momentum is an intrinsic phenomenon of electron. Overall we can consider the total magnetic moment of a particle as its spin and these spins of magnetic materials interact with other spins and with external magnetic field. Thus, on the basis of magnetic interactions, magnetic materials can be divided into diamagnetism, paramagnetism, ferromagnetism, antiferromagnetism and ferrimagnetism.

1.1.1 Diamagnetism:

Diamagnetism is the property of a material or an ion to rectify an applied magnetic field. Lenz's law describes the diamagnetic behaviour of material. According to Lenz's law, for a current loop enclosing a magnetic field, any change in the magnetic flux through the loop will create a current in the loop opposing the change in the flux. Thus, change in any external field causes all atoms to show some degree of diamagnetism. This happens due to orbital

motion of electrons around a nucleus. However, quantum mechanical phenomenon generates the inherent diamagnetism in every material. Diamagnetic material exhibits paired electron. So, they give rises to zero net magnetic moment. These materials show negative susceptibility.

1.1.2 Paramagnetism:

Paramagnetism is the property of a material to align to an applied magnetic field. Paramagnetic materials have unpaired electron so, they possess net magnetic moment and show small but positive susceptibility. In these materials, the spins are randomly orientated in absence of an external field as these spins are merely spin independent. However, on applying an external magnetic field, these spin moments are aligned in the direction of magnetic field. Theoretically, paramagnetism can be described by partition function. The system can be considered as a canonical ensemble which has N free spins in an applied field. The partition function is

$$Z = \sum e^{\beta \mu_i H} \tag{1.1}$$

Where μ_i is the magnetic moment of i ion and β is the Boltzman's constant [1, 2].

The magnetic moment in the j direction

$$\mu_j = g_{jk} S_k \mu_B \tag{1.2}$$

Where, S_k is the total angular momentum of a single ion, g_{jk} is the Lande g's factor, μ_B is Bohr magneton and *k* is the spatial direction [3].

In this way, we can express Curie-Weiss equation as

$$\chi = \frac{M}{H} = \frac{N\mu_B^2 g^2 S(s+1)}{3k_B T} \tag{1.3}$$

Fig. 1.1 shows the spin arrangement of diamagnetic and paramagnetic materials at zero and in presence of magnetic field H.

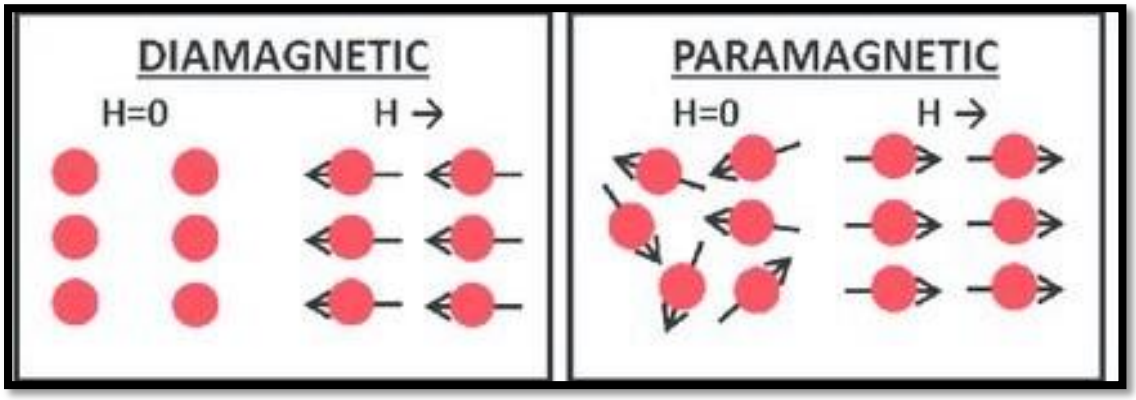

Figure 1.1 : Schematic representation of spin alignment in diamagnetic and paramagnetic materials microscopic structures at rest and in the presence of a magnetic field H.

1.1.3 Ferromagnetism:

The alignment of spin in ferromagnetic material is parallel to their neighboring spins. On applying an external magnetic field, these spins aligned to the direction of magnetic field. These materials have positive and strong magnetic susceptibility. Moreover, ferromagnetic material has inherent property of remnant magnetization i.e. these material retain its magnetic properties even after applied magnetic field switched to zero. Ferromagnetism process can be understood by the formation of magnetic domain. When the free energy of a system minimized, the magnetic domain is formed. In the presence of magnetic field, these materials show hysteresis.

1.1.4 Antiferromagnetism:

The alignment of spin in antiferromagnetic material is antiparallel to their neighboring spins. Thus, they show zero net magnetic moment. As they mutually cancel each other magnetization.

1.1.5 Ferrimagnetism:

Ferrimagnetism possess both ferromagnetism and antiferromagnetism. Because, the spin alignment is similar to antiferromagnetism, while, non zero net magnetization is similar to ferromagnetism. In ferrimagnetic material, the direction of spin is antiparellel to its neighboring spin. But magnetic moment of one sub lattice is higher than the neighboring sub lattice. Thus, it possesses net magnetization. Fig. 1.2 shows the alignment of spins in ferromagnetic, antiferromagnetic and ferrimagnetic materials.

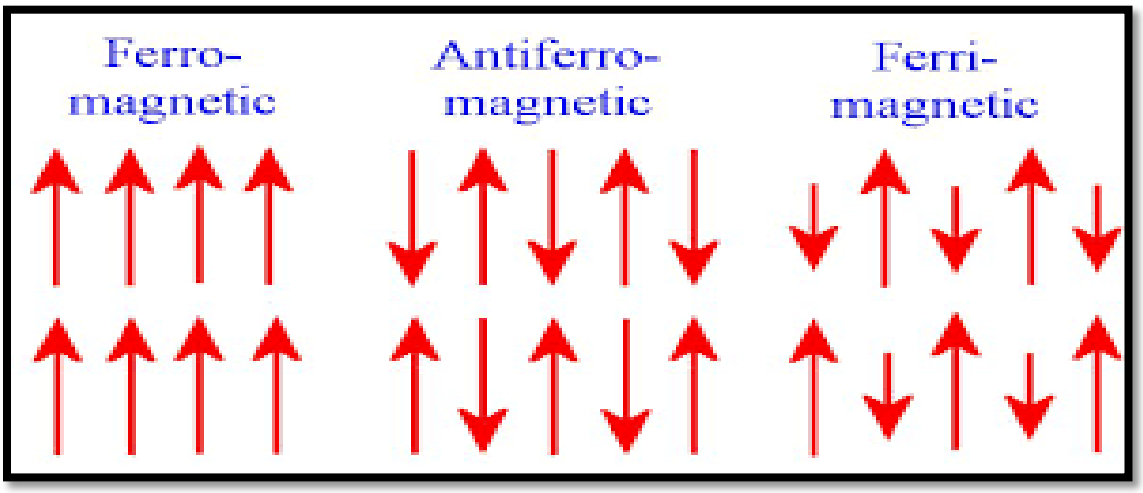

Figure 1.2 : Schematic representation of spin alignment in ferromagnetic, antiferromagnetic and ferrimagnetic materials.

1.2 Rules define the different types of magnetic ordering:

1.2.1 Curie –Weiss Law:

Curie- Weiss law shows the relation between magnetic susceptibility (χ), Curie constant (C), temperature (T) and Curie –Weiss temperature (θ). This law can be stated as

$$\chi = \frac{C}{T-\theta} \qquad (1.4)$$

Curie –Weiss temperature (θ) helps to determine the different type of magnetic ordering exhibited by material. Fig. 1.3 shows the variation of inverse magnetic susceptibility with temperature for different materials.

(i) For paramagnetic materials, $\theta = 0$ K

(ii) For Ferromagnetic materials, $\theta =$ positive value

(iii) For Antiferromagnetic materials, $\theta =$ negative value

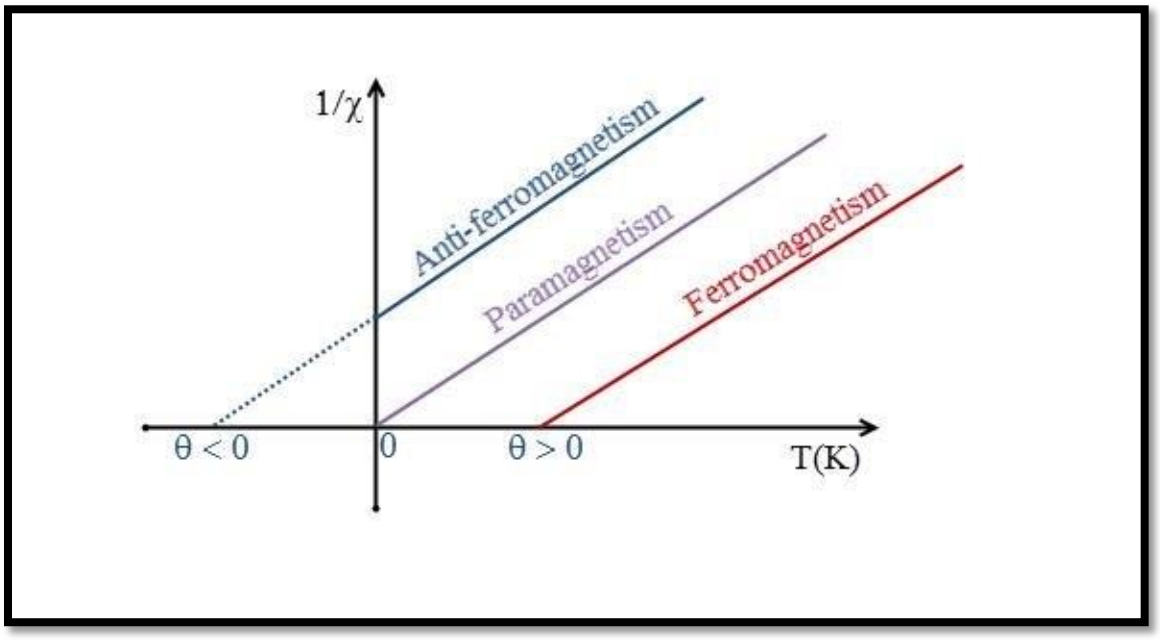

Figure 1.3: Temperature variation of inverse magnetic susceptibility for paramagnetic, ferromagnetic and antiferromagnetic material.

There are also some theories related to magnetism which are

1.2.2 Landau theory of ferromagnetism (mean field theory):

The free energy can be given as

$$F(M) = F_0 + a(T)M^2 + bM^4 \quad (1.5)$$

Where F_0 and b are constants ($b > 0$) and $a\ (T)$ is temperature dependent parameter. The system gives proper transition if $a(T)$ can be shown as

$a(T) = a_0 (T-T_C)$, where a_0 is a proper constant.

To minimize the free energy,

$$\frac{\partial F}{\partial M} = 0 \qquad (1.6)$$

$$2M[a_0(T-T_C)+2bM^2] = 0$$

$$M = 0 \text{ or } M = \pm \left[\frac{a_0(T-T_C)}{2b}\right]^{1/2}$$

The second term is only applicable when $T < T_C$. The first term uses above or below T_C. However, Below T_C, It gives only unstable equilibrium ($\frac{\partial^2 F}{\partial^2 M}$). So, the magnetization (M) follows the curve for $T > T_C$. For $T < T_C$, it is proportional to $(T_C-T)^{1/2}$.

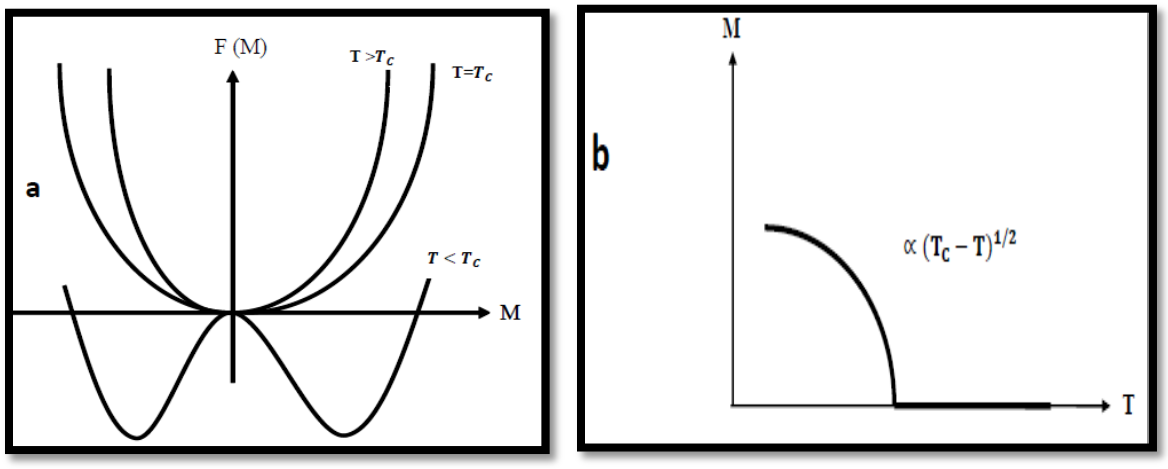

Figure 1.4 (a) Variation of free energy with magnetization. (b) Variation of Magnetization as a function of temperature. [Courtsey: Stephen Blundell, Magnetism in condensed matter; Oxford master series in condensed matter physics]

1.2.3 Heisenberg Model:

By using Heisenberg model, the total energies of different magnetic configurations are written as

$$\mathbf{H} = -\sum_{<ij>} \boldsymbol{J_{ij} S_i . S_j} \quad (1.7)$$

Here, J is exchange constant and S_i and S_j are the pauli matrices. This model is used in the identification of phase transitions and critical points of magnetic system. For these magnetic systems, spins are treated as quantum mechanically.

1.2.4 Ising Model:

The spins are only allowed to point up or down in Ising model. In this model, only z component of spin is being considered. The Hamiltonian of this model is written as

$$\mathbf{H} = -\sum_{<ij>} \boldsymbol{J_{ij} S_i^z S_j^z} \quad (1.8)$$

Here, S^Z is operator for z component of the spin. When the Ising spins are arranged in a one-dimensional lattice, there is no phase transition happened. The Hamiltonian for N+1 spin is

$$H = -2J \sum_{i=1}^{N} S_i^z \; S_{i+1}^z \quad (1.9)$$

1.2.5 Landau theory of phase transition:

This theory is related with the behaviour of ferromagnetism. It is found that near the phase transition temperature T_C, magnetization varies as

$$\boldsymbol{\chi \propto (T - T_c)^{-\gamma}}, \qquad \boldsymbol{T > T_c} \quad (1.10)$$

$$\boldsymbol{M \propto (T_C - T)^{\beta}}, \qquad \boldsymbol{T < T_C} \quad (1.11)$$

$$\boldsymbol{M} \propto H^{1/\delta}, \qquad \boldsymbol{T = T_C} \quad (1.12)$$

Here, β, γ and δ are the critical exponent. These critical exponents yield the information about the nature of phase transition.

Critical exponent of various models:

Exponent	Mean field Model	Ising Model	Heisenberg Model
D	Any	1	3
d	Any	2	3
β	½	1/8	0.367
γ	1	7/4	1.388
δ	3	1.5	4.78

1.3 Spin Frustration:

In nature, every human being wants to live an unperturbed life. However, sometimes a little frustration or perturbation make their life more genuine and relevant. In similar manner, in condensed matter physics, every system wants to achieve some single ground energy state with the lowest overall energy. The third law of thermodynamics also quantified this property. According to this law, entropy of a system goes to zero annd the temperature tends to zero (T→ 0) [1, 2]. However, some versatile systems do not follow third law of thermodynamics and shows multiple degenerate macroscopic ground states. Thus, even at T = 0, these systems may switch in different states. Such amazing systems are known as spin frustrated systems. Spin frustration has been reported in liquid crystals, molecular crystals like solid N_2, in superconducting Josephson junction arrays in a magnetic field and in magnetic thin films. Generally, geometrical spin frustration and disorder driven spin frustration are widely investigated type spin frustration in condensed matter physics.

1.3.1 Geometrical Spin Frustration:

Geometrically spin frustration can be understood by a process in which a system can not satisfy all of its magnetic exchange interactions simultaneously due to crystal lattice geometry. This type of frustration can be explained by classic example of 2 d triangular lattice which is shown in fig. 1.5. In fig. 1.5, we have considered one triangle in lattice which has Isings spins on vertices. The directions of two spins are anti-align, whereas, the third spin has not preferred direction. Thus, it creates degeneracy and shows residual entropy at zero temperature.

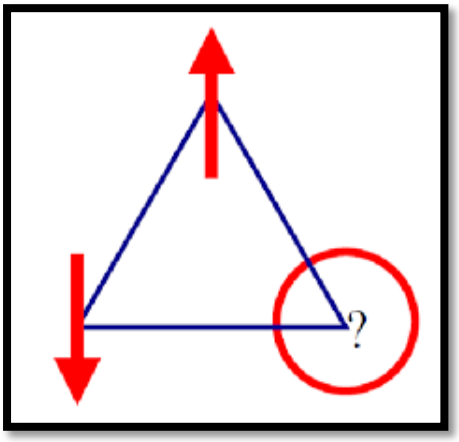

Figure 1.5: Direction of Ising spins on the vertices of 2 d triangular lattice illustrates geometrical spin frustration in which two spins are align antiferromagnetically where as the direction of third spin is not definite.

Considering this 2 d triangular lattice, the Hamiltonian can written as

$$H = - J_{ex} \sum S_i S_j \qquad (1.13)$$

Where J_{ex} is the exchange energy and S_i and S_j are the Ising spins at the i^{th} and j^{th} side (± 1 for up or down).

Case I: when J_{ex} = (+ve) i.e. ferromagnetic case, in this case, all exchange interactions are satisfied by alignment of all spins in up or down direction.

Case II: when J_{ex} = (-ve) i.e. antiferromagnetic case, in this case, only one exchange interactions between two spins are satisfied. The second exchange interactions will forced the

third interaction to be coupled as up and up or down and down spins. In this way, total possible six degenerate magnetic ground states are found as shown in fig. 1.6.

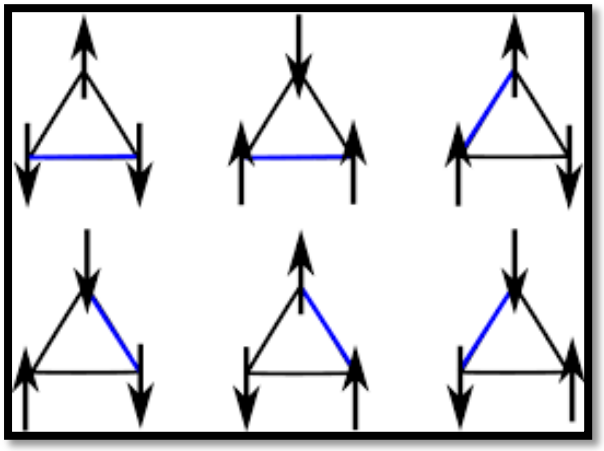

Figure 1.6: Geometrical spin frustration demonstrated six-fold degenerate ground state on the triangular lattice for antiferromagnetic (J_{ex} = -ve).

Therefore, in geometric spin frustration, we can achieve 6 macroscopic ground states, whereas in the case of ferromagnetic system, only 2 ground states can be obtained.

The level of frustration in the magnetic frustrated systems can be measured by frustration index parameter (f). The term 'f' can be defined as [4]

$$f = \frac{|\theta_{CW}|}{T^*} \tag{1.14}$$

Here, θ_{CW} is Curie-Weiss temperature and T^* is critical temperature (T_C) or Neel temperature (T_N). θ_{CW} is defined as the high temperature which calculated from linear part of inverse susceptibility and T^* is the temperature at which long-range spin order develop in the frustrated systems.

For geometrically frustrated system, Ising spins are not necessary. There are some other examples of geometrical spin frustration. Fig. 1.7 shows the various examples of other such types of magnetic lattices.

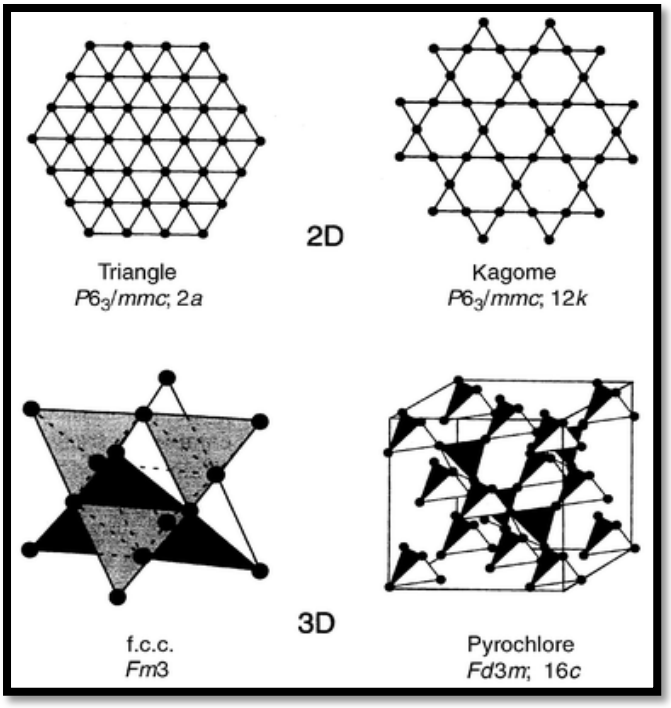

Figure 1.7: Examples of some possible geometrically frustrated magnetic lattices along with their space groups. The top two examples are of two dimensional frustrating lattice geometries, the bottom two examples are of two dimensional frustrating lattice geometries.

Among all these lattices, the 2-d lattices are triangle and kagome lattice, while the 3-d lattices are face-centered cubic (FCC) and pyrochlore lattice. These all lattices have triangular arrangement of spins. As

(i) Triangular lattice has side sharing triangles.

(ii) Kagome lattice has side sharing triangles.

(iii) FCC lattice has side sharing tetrahedra.

(iv) Pyrochlore lattice has side sharing tetrahedra.

Pyrochlore oxide materials with their structure are one of the focuses of this thesis.

1.3.1.1 Pyrochlore oxide materials:

Pyrochlore oxide material is one of the widely explored geometrical spin frustrated material. Pyrochlore material has an empirical formula $A_2B_2O_7$ in which A^{3+} ion is a rare earth element and B^{4+} is a transition element [4]. In such oxides A and B ions are reside on two different interpenetrating lattices of corner-sharing tetrahedral and forms corner-sharing tetrahedral Pyrochlore lattice as shown in fig. 1.8.

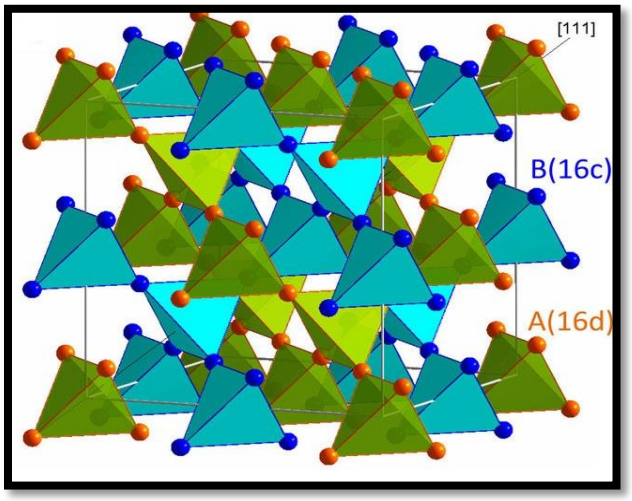

Figure 1.8: Shows the Conventional unit cell of the corner-sharing tetrahedral $A_2B_2O_7$ pyrochlore structure with A^{3+} and B^{4+} sublattices.

The name 'pyrochlore' was taken from the mineral $NaCaNb_2O_6F$ Pyrochlore whose structure was first illustrated by Von Gaertner in 1930 and the meaning of word 'Pyrochlore' is "green fire", thereby these systems are known as 'pyrochlore'. The structure of Pyrochlore contains two cations and one eighth fewer anions. Basically, Pyrochlore structure is derived from the fluorite (CaF_2) type structure. However, fluorite type shows site-disorder as in its structure in which four B^{4+} cations have surrounded an unoccupied interstitial 8a site. Highly ordered Pyrochlore oxides are crystallized into Cubic "$Fd\bar{3}m$" (227) space group [4]. In practice, $A_2B_2O_7$ type is formulated into $A_2B_2O_6O'$. According to crystallography structure,

the B-site ion is reside at 16c (origin of $Fd\bar{3}m$), A-site ion reside at 16d, while O ion placed at 48f and O' ion at 8b. The arrangement of O and O' ion can be clearly seen in fig. 1.9.

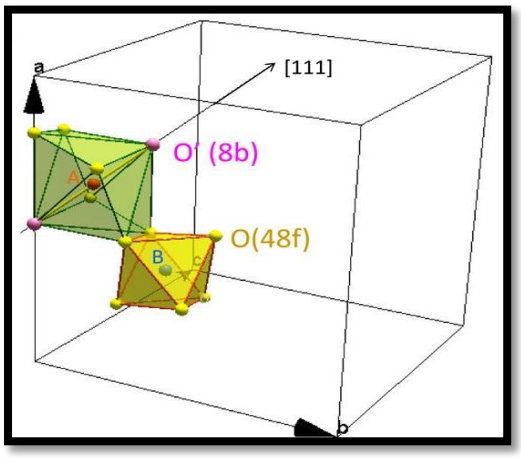

Figure 1.9: Shows the Conventional unit cell of $A_2B_2O_7$ pyrochlore structure with the arrangement of O and O' ion.

The crystallographic positions of cubic $A_2B_2O_6O'$ Pyrochlore are listed in Table 1.

Atom	Wyck off position	Minimal co-ordinates	Point symmetry
A	16d	(1/2,1/2,1/2)	$\bar{3}m$ (D_{3d})
B	16c	(0,0,0)	$\bar{3}m$ (D_{3d})
O	48f	(x,1/8,1/8)	mm (C_{2v})
O'	8b	(3/8,3/8,3/8)	$\bar{4}3m$ (T_d)

Table 1.1: Shows the crystallographic positions of cubic $A_2B_2O_6O'$ Pyrochlore oxide having $Fd\bar{3}m$ space group symmetry.

In this way, both 16c and 16d sites ion form a 3-d arrangement of corner-sharing tetrahedra. In this perspective, it can be seen that stacking of alternating kagome and triangular planar layer which are resultant from 16c or 16d elements at [111] directions, form a Pyrochlore lattice as shown in fig.1.10.

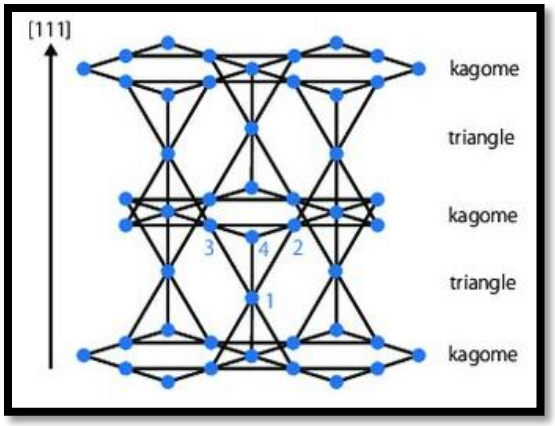

Figure 1.10: Shows the pyrochlore lattice posses alternating kagome and triangular planar layers stacked along [111] direction [4].

Phase stability:

The formation and stability of Pyrochlore phase is an important feature to discuss here. At room temperature, more than 15 tetravalent ions can occupy the B-site of pyrochlore oxide. The A-site reside rare-earth elements forms a series of predominately trivalent states and due to lanthanide contraction, the ionic radius of A-site elements decreases with increasing atomic number (Z). However, it is unusual to realize that stable pyrochlore material has been occurred for all A for a given B. In order to find out the phase stability of pyrochlores with respect to ionic radii ratio of A^{3+} and B^{4+} ion, structure-field map or the structure-stability map has been designed by Subramanian and Sleight in 1993 [4]. This comprehensive map is shown in fig. 1.11.

From this map, it is clear that only Sn element at B-site can form stable pyrochlore phase with all rare earth elements. Thus, stability of pyrochlore phase is determined by the ionic radius ratio of A^{3+}/B^{4+} ions. Here, are the some points which briefly demonstrate the facts of structure stability map of pyrochlore materials.

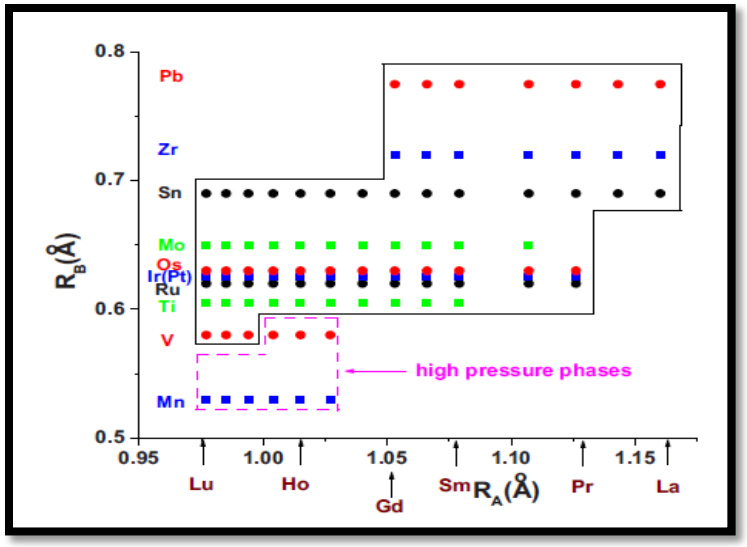

Figure 1.11 : Shows the structural stability map for $A_2B_2O_7$ Pyrochlore.

- For small radii B-ions like Mn^{4+}, only high pressure method has been used for synthesis.
- At ambient pressure, V element at B-site can form stable phase with A-site ions like Lu, Yb and Tm.
- With largest radii B = Pb^{4+} ion, only Gd (smallest rare earth) can form stable Pyrochlore phase.

Hence, the stable pyrochlore phase range at ambient pressure is interpreted in the form of ionic radius ratio (IRR) of A^{3+}/B^{4+} ions which marginally lies between 1.36-1.71. However, there are some exceptions for same, like, $Pr_2Ru_2O_7$ show stable phase for IRR of 1.82, while $Pr_2Mo_2O_7$ with IRR of 1.73 does not form stable phase.

Depends upon stiochiometry, electrical, magnetic and crystallographic properties, pyrochlore material can be divided in four phases.

1.3.1.1.1 Long range ordered:

Long range ordered phase in pyrochlore materials is originated from anisotropic spin-spin interaction, single-ion anisotropy and neighbor exchange interactions. The pyrochlore materials which shows long range ordered phase are $Er_2Ti_2O_7$, $Gd_2Ti_2O_7$, $Tb_2Sn_2O_7$, $Gd_2Sn_2O_7$, $A_2Ru_2O_7$ (A = Y, d, Dy, Ho, Er, Tl), $A_2Mn_2O_7$ (A = Sc, Y, Tb-Lu, Tl), $A_2Ir_2O_7$ (A = Nd to Yb) etc.

1.3.1.1.2 Spin Liquid:

The most dynamic and least ordered phase present in pyrochlore lattice is Spin-liquid phase. From the classical Heisenberg (isotropic) spin model, a "collective paramagnetic" ground state has been predicted by both theoretical calculation and Monte-Carlo simulation for pyrochlore lattice [5-8]. Moreover, quantum Heisenberg spin (S = ½) model also suggested the ground state of pyrochlore like as the 'spin-liquid' state [9]. Therefore, both classical and quantum model describes the term for this state as 'collective paramagnet' and 'spin liquid' respectively which are assigned to have non-trivial short range spin correlated strong ground states. These short range spin arrangements are similar to short range position arrangement in ordinary liquid. Thus, such systems are named as "spin-liquid". Spin liquid compounds do not exhibit long range magnetic order down to temperature T = 0 K. The pyrochlores which undergoes spin liquid state are $Tb_2Ti_2O_7$, $Yb_2Ti_2O_7$, $Er_2Sn_2O_7$ and $Pr_2Ir_2O_7$.

1.3.1.1.3 Spin Ice:

As earlier mentioned, generally antiferromagnetically coupled isotropic Heisenberg spins generate the frustration in pyrochlore lattice. However, some pyrochlore candidates who are

ferromagnetic in nature exhibit frustration. Actually, the orientations of spins in such materials are along an axis [111] which joins the tetrahedron vertices along its centre. In this manner, frustration develops in these system and such pyrochlore materials are commonly known as "Spin-Ice" compound [10, 11]. The term "Spin-Ice" is analogous to water ice as spin ice follows the 'ice-rules' i.e. "Two-in, Two out" arrangement. Fig. 1.12 clearly explains the 'two-in, two-out' arrangement in water ice and spin ice structure [12].

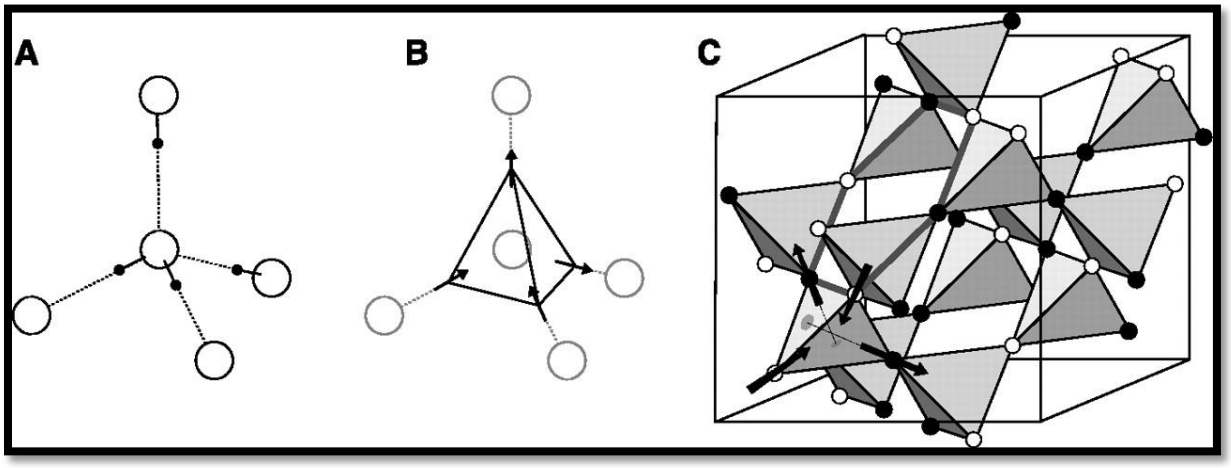

Figure 1.12: Showing the 'two-in, two-out' arrangement as A) In water ice between oxygen (large circle) and Hydrogen atom (black sphere). B) Ice rule follow in a single tetrahedral C) The cubic unit cell of spin ice pyrochlore lattice in which white sphere directs to spins into a 'downward' towards tetrahedra, while black sphere directs to spins 'upwards' towards tetrahedral [12].

According to Pauling's ice water model, the arrangement of oxygen (O) and hydrogen (H) in water (H_2O) molecule as

- One H atom is connected to two nearest neighbor oxygen atoms.
- From the 4 H atoms which surrounded the 1 O atom, 2 H atoms form the covalent bond with the same O atom. Thus, they show "In" arrangement, while rest 2 H atoms covalently bonded with other O atoms. So, they show "out "arrangement. In this way, H and O atoms follow the ice rule. The same analogy has been observed for some pyrochlore lattice in which he arrangement of two spins point "In" of the tetrahedron, while other two spins

point “Out” of the tetrahedron”. As a result, in both cases, system has large number of macroscopic degenerate ground states. There are the reported pyrochlore compound in which ice-rule follow are $Dy_2Ti_2O_7$, $Ho_2Ti_2O_7$, $Pr_2Sn_2O_7$, $Dy_2Sn_2O_7$ and $Ho_2Sn_2O_7$.

1.3.1.1.4 Spin Glass:

Magnetic frustration or some type of chemical disorder originates the spin glass phase [13, 14].

Generally, spin glass phase exhibits in $A_2Mo_2O_7$ (A = Y, Tb) type pyrochlore [4, 15, 16]. The description of spin glass mechanism is explained later in this chapter.

1.3.2 Disorder driven Spin Frustration:

The type of spin frustration which arises due to disorderness in system is known as disorder driven spin frustration. Similar to geometrical spin frustration, disorder driven spin frustration can also lead to various magnetic properties in materials. This disorder driven spin frustration is one of the origin of exotic magnetic properties viz. Exchange Bias (EB), Griffith phase, magneto-dielectric coupling (MDC), metamagnetic transition, low temperature reentrant spin glass (SG) or cluster glass (CG), magneto resistance (MR) etc. in materials [17-28]. However, disorder in a system may be of different kinds like structural disorder, site-disorder or chemical disorder. Generally, perovskite and double perovskite materials exhibit same spin frustration.

1.3.2.1 Single Perovskite Material:

Perovskite material is first discovered by Gustav Rose in 1839 in the Ural mountains of Russia. It named after the name of Russian mineralogist L. A. Perovski. The crystal structure of perovskite material is same as the crystal structure of $CaTiO_3$ (Calcium Titanium Oxide).

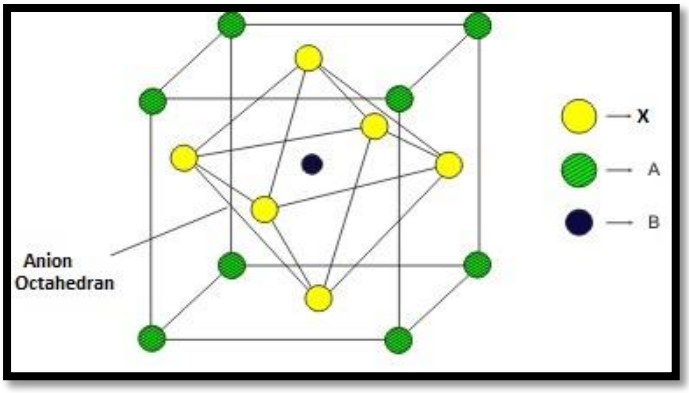

Figure 1.13: Show the crystal structure of ABX_3 perovskite.

The general chemical formula of perovskite material is ABX_3, where A-site ion which resides on the corner of lattice is usually alkaline earth or rare earth element and B-site ion occupies the centre of lattice. Generally, B-site elements are 3d, 4d or 5d transition elements. The X-site anion posses the edge centres of lattice. In this manner, X anions make bond to both A and B cations [29]. The crystal structure of cubic perovskite unit cell is shown in fig. 1.13. However, the cubic or undistorted structure of type compound is rarely survived due to interplay between electron, lattice and spin degree of freedom. Thus, the symmetry is lowered to trigonal, orthorhombic or tetragonal structure.

1.3.2.2 Double Perovskite Material:

From the name 'Double Perovskite (DP)', it is obvious that there should be two perovskite i.e. $ABX_3.AB'X_3$. Thus, it forms a general chemical formula for DP is $A_2BB'O_6$. Two unit cell of single perovskite is alternately repeated in DP crystal structure. Fig.1.14 demonstrates the formation of DP from single perovskite cell.

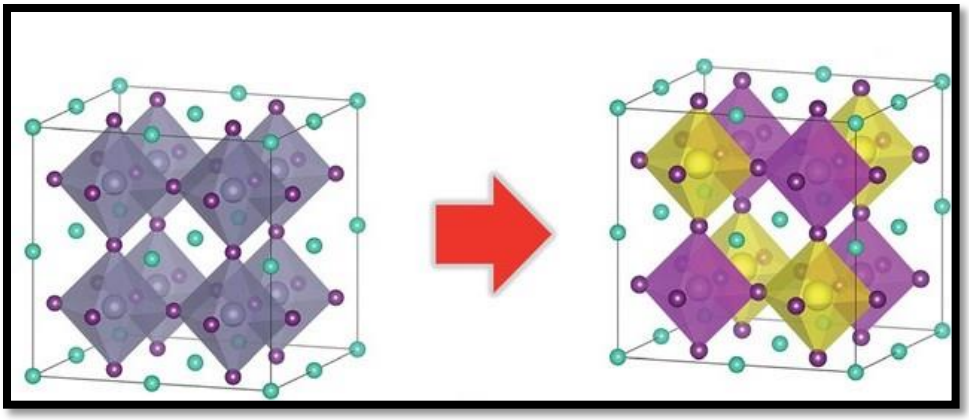

Figure 1.14: Describe the Double Perovskite unit cell structure formed by two perovskite unit cell. In this figure, blue sphere denotes A-site ion, violet sphere denotes B-site ion and yellow sphere presents B'-site ion.

In the DP's unit cell, B and B'-site (transition metal) ions are coordinated with six oxygen atom. So, BO_6 and $B'O_6$ octahedral are repeated in 3-d direction to form a DP structure. In such materials, variable possible combinations of B and B' ions give the rich platform for different magnetic phases like FM, AFM, SG/CG etc. Moreover, ionic radius and valence states of B/B' ions also decide the type of magnetic ordering present in system. If the B/B' ions have different ionic radius and valance states, then it turns to induce FM material by Goodenough-Kanamori Rules [23, 30]. Further, if B^{3+}/B'^{3+} have same ionic states, then it induces AFM in materials by same rule. The geometrical stability of DPs is calculated by Goldschmidt tolerance factor 't' as

$$t = \frac{r_A + + r_O}{\sqrt{2}(\frac{r_B}{2} + \frac{r_{B'}}{2} + r_O)} \quad (1.15)$$

Where, r_A, r_B, $r_{B'}$ and r_O are shannon ionic radius of A, B, B' site and oxygen ions respectively. The inter link of charge and spin make these materials more practical and applicable in daily life. The research areas for such materials are wide due to their functionality as they are useful in electronics as well as in magnetism.

1.4 Literature survey on $A_2Ti_2O_7$ type Pyrochlore materials:

Among Pyrochlore world, rare earth titanates ($R_2Ti_2O_7$) have well known and prominent pyrochlore society. In such pyrochlore, only rare earth element R^{3+} is magnetic element as both Ti^{4+} ($3d^0$) and O^{2-} (filled shell $2s^22p^6$) are diamagnetic. Crystalline electric field determine the Hamiltonian for theses material, which stated as,

$$H_{CF} = \sum_i B_l^m \sum_{i,m} O_l^m (J_i) \quad (1.16)$$

Here, J_i is angular momentum operator, B_l^m *is* crystal field parameter and O_l^m is Stevens operator equivalents [4]. Here, is the brief discussion of fascinating $R_2Ti_2O_7$ pyrochlores which attracts the attention of researchers towards themselves.

- **$Er_2Ti_2O_7$ System**

Erbium titanate ($Er_2Ti_2O_7$) is a well-known XY antiferromagnate pyrochlore in which crystal field ground state of Er^{3+} single ion is a Kramer's doublet. As a result, it possess magnetic moment of 0.12 μ_B and 3.8 μ_B parallel and perpendicular to <111> axis respectively. Moreover, above the ground state, the lowest lying crystal field states has been observed at 6.38 meV (74.1 K) and 7.39 meV (85.8 K) for $Er_2Ti_2O_7$ [31].

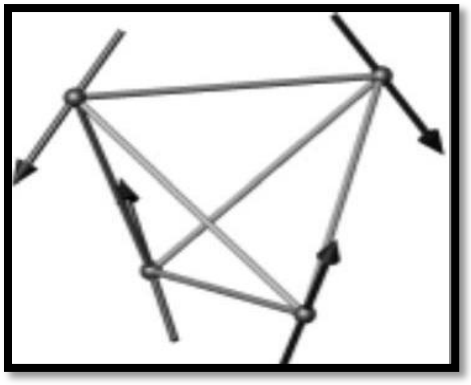

Figure 1.15: Shows the ground state spin configuration achieved for $Er_2Ti_2O_7$ [32].

The negative Curie-Weiss (CW) temperature (θ_{CW} = ~ -22 K) and value of critical exponent ($\beta \approx$ 0.33) extracted from neutron scattering data validates the XY antiferromagnetic material of $Er_2Ti_2O_7$ [31]. Moreover, specific heat and neutron diffraction measured that $Er_2Ti_2O_7$ shows long range antiferromagnetic ordering represent as ψ_2 basis vector of Γ_5. Along with, it undergoes a second order phase transition [32]. This peculiar feature of system is owned by thermal fluctuations and quantum order-by disorder process. Thereafter, frequency dependent AC susceptibility observed two unusual and distinct spin relaxations in $Er_2Ti_2O_7$ [33]. Recently, these both mechanisms are named as an Orbach process which consists cross-tunneling and phonon bottleneck effect.

- **$Gd_2Ti_2O_7$ System**

Gd^{3+} ion (S=7/2) in $Gd_2Ti_2O_7$ which has zero orbital momentum and half filled 4f is one of the Heisenberg spin examples in Rare earth ions. It is well known fact that antiferromanetically coupled Heisenberg spins which reside on pyrochlore lattice are highly frustrated as they can minimize the exchange energy in different ways [34]. Fit of Curie-Weiss law on DC susceptibility data of $Gd_2Ti_2O_7$ gives the negative CW (θ_{CW} = ~ -10 K) and effective magnetic moment ~ 7.94 μ_B [34, 35]. Raju et.al and Ramirez et.al reported that on measuring with AC susceptibility and neutron diffraction, this system has entered into two magnetic transitions at 0.97 K and 0.7 K [36, 37]. The transition at 0.97 K is observed in zero magnetic field whereas, transition at 0.7 K is observed in presence of magnetic field.

- **$Tb_2Ti_2O_7$ System**

As being rare earth titanate, only Tb^{3+} ion is magnetic ion in $Tb_2Ti_2O_7$. Temperature dependent DC magnetic susceptibility data of system yielded the information of negative CW temperature (θ_{CW} = ~ -19 K) and effective magnetic moment (~ 9.6 μ_B/Tb) [38]. One of the

attractive feature of $Tb_2Ti_2O_7$ compound is that system does not undergoes any long range ordering even below at T~ 50 mK and remains in spin liquid state [39]. However, theoretical study in terms of crystal field effect of Tb^{3+} and dipolar and exchange interactions of compound suggested a transition at ~1.8 K in which system shows a long range ordering with a random phase approximation [40]. Inelastic neutron scattering depicted the two singlet spin-liquid states in this pyrochlore. The mentioned property is surprising because Tb^{3+} is a non-Kramer's ion [41, 42]. Further, theoretical study on such ground states predicts the possibility of quantum spin ice as well as quadruple ordering in system [43, 44]. Moreover, $Tb_2Ti_2O_7$ also shows a field induced transition at low temperature due to single moment saturation [45]. The spin liquid sate in $Tb_2Ti_2O_7$ is also confirmed by temperature dependent Raman spectroscopy. Mączka et. al. reported that $Tb_2Ti_2O_7$ shows correlated interactions between the phonons and crystal field leads to spin liquid state [46]. Recent study on $Tb_2Ti_2O_7$ reveals the transition from metal to insulator at 603 K. The transition is observed in resistivity Vs. temperature curve due to interaction between empty 3d orbitals of Ti^{4+} and O^{2-} ions [47].

- **<u>$Yb_2Ti_2O_7$ System</u>**

Ytterbium titanate ($Yb_2Ti_2O_7$) is a ferromagnetic insulator with θ_{CW} = ~ 0.59 K and magnetic moment = 3.3 μ_B[4]. The Moosbauer spectroscopy on the system determined the energy separation of about 620 K between the first excited state to ground state under crystal field scheme. This behaviour presents the easy plane X-Y anisotropy in $Yb_2Ti_2O_7$ [49]. Specific heat and neutron diffraction measurement revealed a first order magnetic phase transition around ~ 0.21 K in the same system [50, 51]. Moreover, slow spin relaxation was observed below this transition temperature. Single crystal of $Yb_2Ti_2O_7$ manifests a change

from magnetic coulomb liquid state to a ferromagnetic state which is commonly known as 'Higg's transition' [52]. Recent studies on $Yb_2Ti_2O_7$ labels this system more special among pyrochlores as quantum spin ice phase has appeared in same one [50-52].

- **$Dy_2Ti_2O_7$ System**

In Dysprosium titanate, Dy^{3+} (J = 15/2) is a Kramers ion whose magnetic moment is 9.7 μ_B. On being spin ice compound, $Dy_2Ti_2O_7$ exhibit residual entropy. Specific heat measurement on $Dy_2Ti_2O_7$ revealed the value of spin entropy is about ~ 0.67 Rln2 which is nearly close to entropy of common ice ~0.71Rln2 [53]. Moreover, Dy^{3+} spins are highly uniaxial along <111> axis in $Dy_2Ti_2O_7$ lattice due to single ion anisotropy. Thus, $Dy_2Ti_2O_7$ exhibits macroscopic degenerate ground state at very low temperature (T< 4K). However, this rule is followed by all other spin materials like $Ho_2Ti_2O_7$, $Dy_2Sn_2O_7$, Ho_2SnO_7 etc. From magnetic susceptibility data, the θ_{CW} for $Dy_2Ti_2O_7$ is ~1 K and dipolar interaction (D_{nn}) is about 2 K. Thus, the dipolar interactions between the spins is ferromagnetic, as a result, effective nearest neighbor interaction between the Dy^{3+} spins is ferromagnetic. Hence, it explains the spin ice behaviour. However, all the spin ice materials show low temperature spin ice freezing at $T_i \sim T_{ice} \sim$ 4 K. Surprisingly, $Dy_2Ti_2O_7$ is only a spin ice candidate which shows high temperature single ion spin freezing (T_f ~16 K) along with spin ice freezing. Moreover, the interconnection of T_i and T_f by a quantum tunneling crossover process from the crystal field barrier, make the $Dy_2Ti_2O_7$ is most promising and widely studied material [53-57].

- **$Ho_2Ti_2O_7$ System**

Dipolar spin ice $Ho_2Ti_2O_7$ has Ho^{3+} [J = 8] as magnetic ion whose magnetic moment is 10.6 μ_B [58-61]. The positive CW (θ_{CW} = ~ 1.9 K) of $Ho_2Ti_2O_7$ promotes the ferromagnetic

spin-spin correlations which induces the exchange interaction strength of about ~ 1 K among Ho^{3+} spins. Being a spin ice material, the energy separation between single ground state $|J, M_J\rangle = |8,\pm 8\rangle$ and first excited state is ~ 20.4 meV or ~ 240 K [60-61]. From the high temperature series expansion fit, the derived values of dipolar energy (D_{nn}) and nearest neighbor exchange energy (J_{nn}) of $Ho_2Ti_2O_7$ compound are ~ +2.4 K and ~ -0.5 K respectively [58, 59]. Similar to $Dy_2Ti_2O_7$, Ho^{3+} spins in $Ho_2Ti_2O_7$ freezes below ~1 K in randomly, non-collimated and disordered fashion. However, unlike $Dy_2Ti_2O_7$, $Ho_2Ti_2O_7$ does not exhibit high temperature spin freezing. There is a report by Ehlers et. al gives the evidence of transition near 15 K in $Ho_2Ti_2O_7$ by neutron spin eco technique [61]. But, this result hindered by low temperature spin ice freezing. May be presence of external magnetic field reveals the transition for $Ho_2Ti_2O_7$ compound.

- **$Sm_2Ti_2O_7$ System**

It is known fact that when the ferromagnetic (FM) dipolar interaction dominates over the antiferromagnetic exchange interaction, the ground state of system is spin ice state (two in two out) arrangement of spins. However, when the AFM exchange interaction dominates over FM dipolar interaction, an 'all in-all out' (AIAO) antiferromagnetic order can be achieved [62, 63]. Recently, same spin configuration (AIAO) has been reported in $Sm_2Ti_2O_7$ pyrochlore [64]. Fig. 1.16 shows the AIAO configuration of Sm^{3+} spins. Alternating corner sharing tetrahedral having the Sm^{3+} spins are arranged directing inwards and all Sm^{3+} spins are arranged directed outwards.

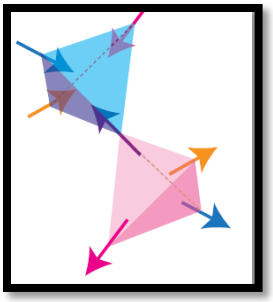

Figure 1.16: Showing the all in-all out spin arrangement in $Sm_2Ti_2O_7$.

Neutron diffraction data of $Sm_2Ti_2O_7$ confirmed that Sm^{3+} spins are antiferromagnetically coupled and having negligible dipolar interaction. Thus, it forms an AIAO configuration.

- **$Eu_2Ti_2O_7$ System**

Europium titanate is one of the focus systems of present thesis. $Eu_2Ti_2O_7$, an X-Y antiferromagnet, exhibits single ion anisotropy (SIA) [65]. In $Eu_2Ti_2O_7$ unit cell structure, 8 O atoms surrounded a Eu^{3+} ion which yielded a trigonally distorted cube with 3-fold inversion (D_{3d}) symmetry. So, this D_{3d} symmetry along with crystal field effect generates the different magnetic ion susceptibility which is along and perpendicular to D_{3d} axis. This result from SIA in same system, electronic pattern of Eu^{3+} ions showed that there is a little difference between the non magnetic ground state ($^7F_0$) and first excited state ($^7F_1$). The first excited $^7F_1$ states further spitted into a single and double state due to crystal; field splitting. Thus, in spite of a non magnetic ground state, it shows the magnetization or magnetic moment. The DC susceptibility study also validates the presence of crystal field effect below 68 k by showing a plateau region in DC susceptibility curve [66]. Recently AC susceptibility measurement on $Eu_2Ti_2O_7$ observed the single ion freezing at T = 35 K [67]. Presence of such high temperature spin freezing in $Eu_2Ti_2O_7$ makes this material auspicious candidate among pyrochlores.

1.5 Literature survey on A_2CoFeO_6 type Double Perovskite:

As matter of fact, intense research and large investigation has been reported for $A_2(Co/Mn/Ni)O_6$ type double perovskites (DPs). Hence, in present thesis, we have centered on less studied DP i.e. A_2CoFeO_6 type DPs. Here is the brief discussion of some reported A_2CoFeO_6 type DPs.

- **La_2CoFeO_6 System**

The Lanthanum (La) ion as A-site element has widely exploited element in double Perovskite family. The La_2CoMn/NiO_6 based DP is one of the most studied materials in research area. The La_2CoFeO_6 (LCFO) is an antiferromagnetic insulator. It shows a long range antiferromagnetic ordering at T_N = 270 K. The system exhibits a low temperature structural change from Rhombohedral ($R\bar{3}C$) at 300 K to orthorhombic (Pnma) at 200 K [68]. This structural transition generates the thermal hysteresis and large irreversibility in compound. The density functional theory (DFT) also verified its insulating non-compensated antiferromagnetic structure. The neutron diffraction data indicates the G-type antiferromagnetic ordering for LCFO system [68]. The isothermal magnetization curve of LCFO yielded the magnetic moment of $\approx 0.2\mu_B$/f.u. recorded at 5 K. However, Monte Carlo computation suggested the space group I4/mmm space group [69].

- **Pr_2CoFeO_6 System**

The DP Pr_2CoFeO_6 (PCFO) is one of the ravishing materials which consists almost all the magnetic phenomenon. Its electronic state study from the XAS and XPS tool reveals the same trivalent (+3) oxidation state for both Co and Fe ion [70, 71]. Absence of any electronic states across the Fermi level indicates the insulating nature of PCFO sample. Moreover, neutron diffraction and magnetization data gives the information of antiferromagnetic

transition at T_N = 269 K. A strong spin-phonon coupling has also addressed for this material [70]. The B-site disordered orthorhombic (Pnma) structure has been adopted for PCFO. The observation of multiple magnetic phases like exchange-bias effect, Griffith phase, long range antiferromagnetic ordering, and reentrant cluster glass (T_G~34 K) make this system highly promising [71]. Along with such magnetic phases, PCFO system also exhibits G type canted AFM spin ordering. In the structure of PCFO, Fe^{3+} spins are canted from their position due to Dzyaloshinsky-Moriya (D-M) interaction.

- **Sr_2CoFeO_6 System**

In view of application purpose, The Sr_2CoFeO_6 (SCFO) DP is one of a strong candidate. Absence of any rare earth element in compound enriches its properties. The ferromagnetic metallic system of SCFO possesses a tetragonal structure with I4/m symmetry without any structural transition. The magnetic ground state for this system is reported as spin glass at T_G~75 K [72]. Mixed valance states of Co ion and antisite disorder present in SCFO induces not only the spin glass phase but also the large magneto-resistance (MR). SCFO material showed the 63 % large MR at 14 K in presence of 12 T magnetic field. Spin scattering of localized carrier due to spin glass state causes such large MR in SCFO [73]. Exchange Bias and memory effect also present in same DP [74].

- **$LaSrCoFeO_6$ System**

The substitution of La ion on Sr site enhances the qualities of SCFO DP. As, $LaSrCoFeO_6$ (LSCFO) DP has a correlation of LCFO and SCFO compounds. Low symmetry monoclinic with $P2_1/n$ space group crystal structure of LSCFO is determined by X-ray diffraction (XRD). Antisite disorder originates a spin glass state at T_G~72 K in LSCFO. Moreover, a giant intrinsic exchange Bias field (~1.2 kOe) has also been reported for this DP

[75]. LSCFO system exhibits a negative MR (~ 47%) at 5 K in presence of 5 T magnetic field [76]. Further, thermoelectric power has also observed in LSCFO sample [77].

- **Ho_2CoFeO_6 System**

Ho_2CoFeO_6 (HCFO) is less studied DP. However, an orthorhombic Pbnm crystallography structure has reported for this system. The temperature dependent magnetization data show two anomalies near T~270 K and T~45 K. The first transition indicates the antiferromagnetic transition from paramagnetic state, while, second transition is identified as spin reorientation transition (T_{SR}) [17]. In HCFO compound, The Fe^{3+} spins are rotate from one axis to another axis by Dzyaloshinsky-Moriya (D-M) interaction. Moreover, Ho^{3+} spins are also contributed in magnetization data as a short range interaction below 5 K. This system possess magneto-dielectric coupling in two different temperature region. In first region, $10< T < 45$ K, the HCFO exhibits MD effect due to interaction between Fe^{3+} and Ho^{3+} spins. Whereas, for second high temperature region (150-300 K), HCFO shows MDC due to grain boundary contribution [78].

Here is the list of some more A_2CoFeO_6 type Double perovskite which required attention to explore their features as they are least studied DP till now.

- Sm_2CoFeO_6
- Gd_2CoFeO_6
- Eu_2CoFeO_6
- Dy_2CoFeO_6
- Er_2CoFeO_6

There is also a brief tabular form of literature survey of $A_2Co/Mn/NiO_6$ type double perovskite materials which are widely investigated.

S N	EXAMPLES	STRUCTURE	ORDERING TEMPERATURE	CHARACETISTICS
1	**La_2CoMnO_6**	Monoclinic ($P2_1/n$)	T_C ~ 225 K	• Ferromagnetic insulator • Large magneto-caloric effect • Magneto-dielectric coupling • Thermoelectric properties • ~ 80% Magneto resistance [79-84]
2	**La_2NiMnO_6**	Monoclinic ($P2_1/n$)	T_C ~ 270 K	• Ferromagnetic insulator • ~16% Magneto-dielectric coupling at 270 K • Ferroelectricity • Spin-phonon coupling • Magneto resistance [55, 85-87]
3	**Y_2CoMnO_6**	Monoclinic ($P2_1/n$)	T_C ~ 80 K	• E type spin ordering • Meta-magnetism • Spin-phonon coupling [88-92]
4	**Y_2NiMnO_6**	Monoclinic ($P2_1/n$)	T_C ~ 81 K	• E type antiferromagnetic spin ordering • Spin-phonon coupling [93-96]
5	**Pr_2CoMnO_6**	Monoclinic ($P2_1/n$)	T_C ~ 178 K	• Ferromagnetic insulator • Griffith-phase • Exchange bias • Magneto-dielectric coupling • Spin-phonon coupling

				[97]
6	**Pr_2NiMnO_6**	Monoclinic ($P2_1/n$)	T_C ~ 208 K	• Ferromagnetic insulator • Spin-phonon coupling [98, 99]
7	**Dy_2CoMnO_6**	Monoclinic ($P2_1/n$)	T_C ~ 85 K	• Meta-magnetic transition • Magneto-caloric effect [100]
8	**Sm_2CoMnO_6**	Monoclinic ($P2_1/n$)	T_C ~ 135 K	• Ferromagnetic insulator • Meta-magnetic transition • Ferroelectric Polarization [101]
9	**Sm_2NiMnO_6**	Monoclinic ($P2_1/n$)	T_C ~ 156 K	• Ferromagnetic insulator • Reentrant spin glass • Positive and negative magneto-dielectric [102, 103]
10	**Gd_2CoMnO_6**	Monoclinic ($P2_1/n$)	T_C ~ 112 K	• Magneto-caloric effect • Observation of Hopkinson effect • Spin-phonon coupling [104-109]

11	**Gd_2NiMnO_6**	Monoclinic ($P2_1/n$)	T_C ~ 134 K	• Griffith-phase • Magneto-caloric effect • Magneto-dielectric coupling • Spin-phonon coupling [110, 111]
12	**Tb_2CoMnO_6**	Monoclinic ($P2_1/n$)	T_C ~ 98 K	• Meta-magnetic transition • Magneto-caloric effect [112, 113]
13	**Tb_2NiMnO_6**	Monoclinic ($P2_1/n$)	T_C ~ 111 K	• Griffith-phase • Spin-phonon coupling [21]

Table 1.2: Shows the characteristics of different $A_2Co/Mn/NiO_6$ type double perovskite materials.

1.6 Different Physical Phenomena related to our research:

1.6.1 Spin relaxation or Spin freezing Process:

When an external field applied in the system, the torque is generated due to the interaction between spin and applied field. The same torque relaxes the spin of system when it aligns with field. The magnetization in DC (static) magnetic field for N identical and non-interacting spins can be given as

$$h\frac{dM}{dt} = -g\mu_B S \times H \tag{1.17}$$

If the field is applied in z direction, them the direction of equilibrium magnetization (M_0) will be in z direction. If an additional field is applied in z direction for finite interval of time and then it is removed, system goes back or relaxes to its original equilibrium. This process will take some finite time of length. However, the condition to gain original equilibrium is that apply external field is just enough to produce a different macroscopic state. But, if the additional field is applied periodically at a frequency whose length of time faster than the relaxation time of the thermodynamic spins system, system remains in a non- equilibrium position. As a result, the obtained value of magnetization is less than M_0. Thus, eq. (1.17) turns to a Bloch equation after adding a sinusoidal small perturbing field to eq. (1.17) [114]. For this case, Bloch equation reduces into eq. (1.18)

$$h\frac{dM_Z}{dt} = g\mu_B(M \times H)_Z \ + \chi_0 \frac{H_1 Cos\omega T - m_Z}{T_1} \tag{1.18}$$

Here, m_Z is component of magnetization in z direction, ω is perturbing field frequency, χ_0 is static susceptibility and T_1 is longitudinal relaxation time of system [115].

The same scenario can be achieved by CW law which yield the information of χ_{DC} (static or DC) susceptibility. This law is valid when the $\chi_{DC} = \chi_T$ (isothermal susceptibility). χ_T is the susceptibility when the temperature of spins and the lattice in which they are embedded are the same. While, if we consider that the lattice and the spin are two different system, then χ_S (adiabatic susceptibility) can be described as the susceptibility when there is no exchange of heat between the lattice and the spin. The AC susceptibility measurement can probe the spin dynamic of the system. On applying a time varying small sinusoidal perturbed longitudinally on material, we can observed the spin relaxation of the system.

From the Casimir-du-Pre-relation [116], the χ_S and χ_T can be written in form of

$$\chi' = \chi_S + \frac{\chi_T - \chi_S}{1+\omega^2\tau_1^2} \tag{1.19}$$

$$\chi'' = \frac{(\chi_T - \chi_S)\omega\tau_1}{1+\omega^2\tau_1^2} \tag{1.20}$$

As already mentioned in this thesis, χ is complex quantity. Hence χ' is real part which is in the phase of applied external field oscillating with ω angular frequency and χ'' is an imaginary part which is 90^0 out of phase to the field. τ is the relaxation time of spin lattice. Fig. 1.17 depicts a graphical representation of real and imaginary part of susceptibility in terms of χ_S and χ_T. Inset of fig. 1.17 shows the phasor relation of χ.

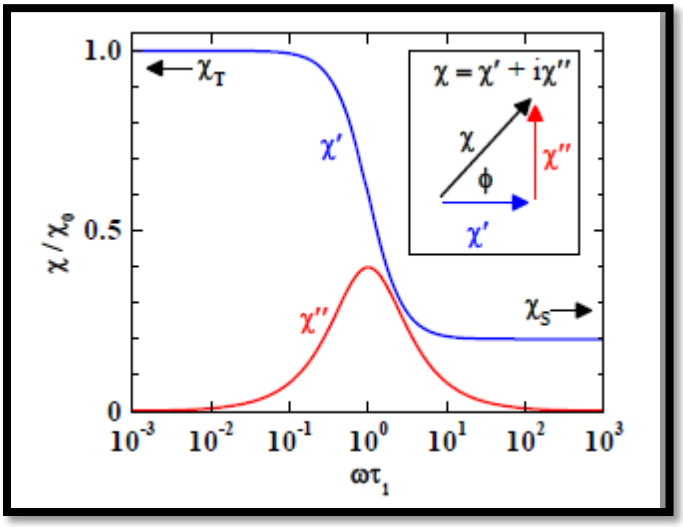

Figure 1.17: The frequency varying real and imaginary part of χ. χ_T and χ_S occur at lowest and highest frequencies respectively. Inset of fig.1.17 demonstrate the phasor diagram of χ. Here, ψ is the phase difference.

However, both real and imaginary part of χ must follow the Kramer-Kronning relation [117, 118]. The separate lattice and spins system assumption is valid in the case if there is a large difference in time scales of spin-spin and spin-lattice relaxation. At low temperature, it is typical because the orbital angular momentum (L) time becomes too large as compared to the relaxation time of spin lattice at low temperature. This large difference in both relaxation times associate with the density of states of both systems. Moreover, lattice of a system alters the orbital angular momentum (L), not the spin angular momentum (S) as S exists in other

space. Lattice can only interact with S by the spin-orbit coupling. Hence, spin-spin is independent of spin lattice reaction [119]. Therefore, it is clear that exchange and dipolar interactions devloples the spin-spin relaxation in system.

1.6.2 Dzyaloshinsky-Moriya (DM) interaction:

Indirect exchange interaction between the spins can be explained by the coupling through any indirect media i.e. it may be conduction electrons, oxygen anions or spin –orbit interaction. The Dzyaloshinsky-Moriya (DM) interaction or anisotropic interaction is one kind of indirect exchange interaction. It leads the action in which total magnetic exchange interactions between two neighboring spins take part [120]. This interaction can be understood by process of super exchange interactions in which two magnetic ions are connected by oxygen ions. However, the role of oxygen ion in DM interaction is played by spin-orbit coupling. Through DM interaction, excited state of one ion is interacted with ground state of other ion. The spin-orbit interaction is excited the state of one magnetic ion in this interaction. Fig. 1.18 demonstrates the DM interaction between spins.

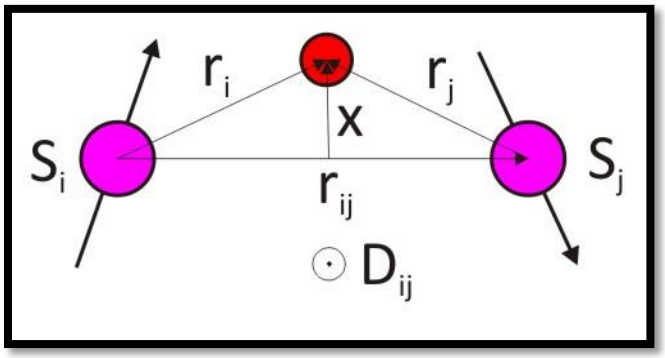

Figure 1.18: Shows the DM interaction between two neighboring spins.

If we considered two spins S_1 and S_2 which are interacted through DM interaction, then the Hamiltonian can be expressed as with an extra term

$$H_{DM} = \vec{D}.\overrightarrow{S_1} \times \overrightarrow{S_2} \quad (1.21)$$

Here, $\vec{D}$ is a vector quantity. The $\vec{D}$ vectors depend upon the symmetry i.e. it lies along the parallel or perpendicular direction to the line connecting the two spins. However, for "inversion symmetry", vector $\vec{D}$ vanishes. DM interaction ensures that the energy of system should be negative. Thus, it attempts to orient the S_1 and S_2 spins at right angle to each other in a plane which is perpendicular to the direction of vector$\vec{D}$. In this way, DM interaction induces the spins to be canted by small angle. This generates a weak ferromagnetism in an antiferromagnetic sample. Generally, the source of ferromagnetism in an orthoferrite antiferromagnetic system is the DM interaction i.e. canting of Fe spins.

1.6.3 Spin-glass/ Cluster glass phenomenology:

Spin glass (SG) state can be referred as a state, in which the magnetic moments of systems are not arranged periodically. Randomness is present in the system. In such state, there is a cooperative and random spin freezing occurs below a definite temperature T_f [120]. The fashion of randomly arrangement of spins in SG state is similar to arrangement of atoms in normal glass. In both cases, there is a lack of periodicity. Spin glass state emerges in a system due to competition between FM and AFM states. Surprisingly, in FM and AFM states, spins are arranged in a regular pattern. But this is totally different for spin glass state. It can be seen in fig. 1.19.

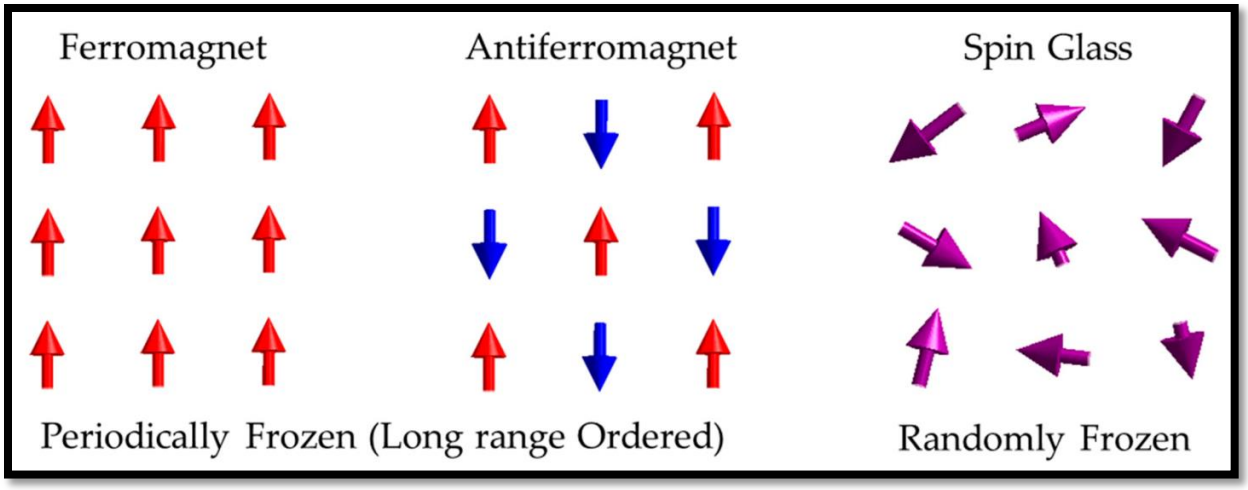

Figure 1.19: Depicts the spin arrangement in ferromagnetic, antiferromagnetic and spin glass state.

Moreover, geometrical frustration and structural disorder are also the origin of such state in systems [121-123]. In SG state, the domain walls of FM/AFM are pinned by disorder in system. So, domain wall in metastable state can reach one state to another state by means of thermally activated hopping. As a result, system does not attain an equilibrium state in given experimental time scale. Thus, the system turns to in magnetic glassy phase with slow spin relaxation. However, the scenario is different for cluster glass state (CG). In CG state, the disorder or spin frustration is present in small area of clusters [124-126]. When the contribution of one component (FM/AFM) is relatively more than another component (AFM/FM), the system undergoes to CG state. Therefore, a cluster of spins relaxes instead of atomic spins. In such cases, cluster of spins can be taken as giant magnetic moment. Fig. 1.20 represents the difference between SG and CG states.

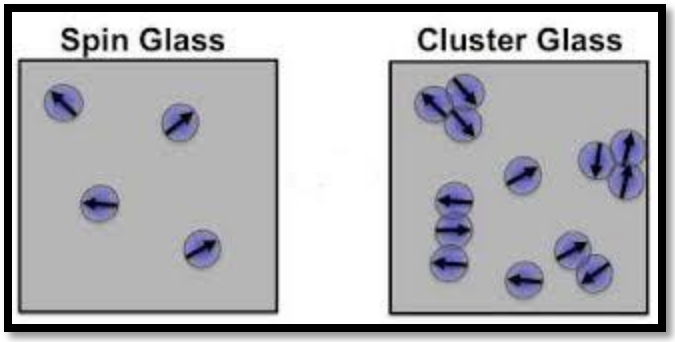

Figure 1.20: Depicts the arrangement of spins in spin glass state and cluster glass state.

From fig. 1.20, it is clear that, a cluster of spins relaxes in CG state, while for SG state, atomic spins relaxes. When a sample exhibits a long range magnetic ordering at high temperature and on lowering the temperature, it turns to a glassy state, the system called to be having reentrant glass state. The models which were given by Sherrington- Kirkpatrick (for Ising spin systems) and Gabay and Toulouse (for Heisenberg spin systems) demonstrate the complexity of reentrant glassy phase [127, 128]. AC susceptibility measurement with a very small time dependent alternating magnetic field identifies the glassy mechanism present in a system. The real (χ') and imaginary (χ'') part of χ_{AC} shows a frequency dependent relaxation peak. Here, are the various laws which determine the parameters of SG/CG state accompanying with frequency dependent χ_{AC}.

a) Mydosh dynamic scaling Power law:

This law can be written as

$$f = f_0 \left(\frac{T_f - T_{SG}}{T_{SG}}\right)^{z\nu} \tag{1.22}$$

where, zν is the dynamical critical exponent, T_{SG} is spin glass (SG) freezing temperature and τ_0 is spin flipping time (τ_0)= $\frac{1}{f_o}$. The value of zν lies between 4 to12 for the glassy state [124, 126]. The parameter which differentiates between the CG/SG states is the value of τ_0 .

(i) For SG: τ_0 lies between ~ 10^{-12} - 10^{-13} s.

(ii) For CG: τ_0 lies between ~ 10^{-4} - 10^{-7} s.

b) Vogel-Fulcher (VF) law:

VF law gives the information about inter-cluster interaction. This law is empirically interpreted as

$$f = f_0 \exp(-\frac{E_A}{K_B(T_f - T_0)}) \quad (1.23)$$

where, K_B is Boltzmann constant, T_o is vogel - future temperature and E_A is activation energy. Eventually, and T_o is also known as inter-cluster interaction strength [129].

1.6.4 Exchange Bias (EB) effect:

When there is a shift of hysteresis loop of a system along the magnetic field axis (H), the system said to be possess Exchange-Bias (EB). This effect can be seen in fig. 1.21.

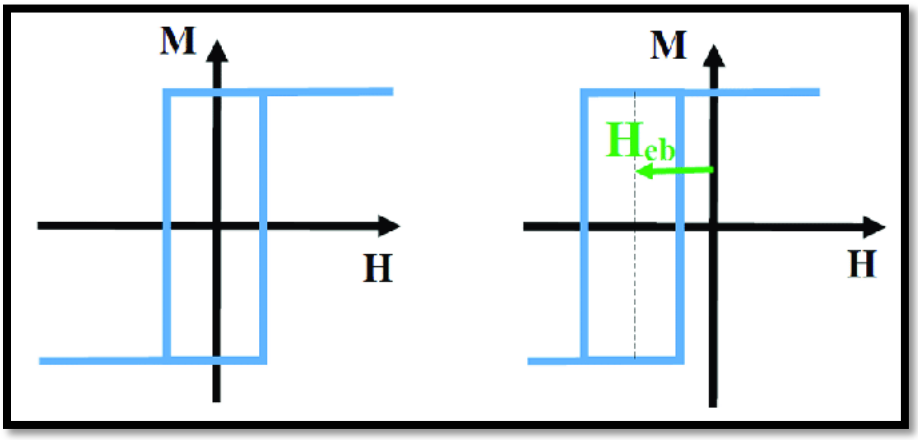

Figure 1.21: Represents the symmetric and asymmetric hysteresis loop in M-H curve.

The asymmetry in M-H curve reflects the Exchange-Bias effect. Meiklejohn and Bean have firstly discovered EB effect in 1956 [130-133]. They observed a hysteresis shift in CoO antiferromagnetic oxide. EB effect can be achieved in the system which has coexistence of various inhomogeneous magnetic phases. The multiple coexisted magnetic phases may be

hard/soft phase of FM, FM/AFM, FM/pin glass, FM/ferrimagnet etc [134-136]. Now –a – days materials which possess EB can be applied in different areas like spintronics, high density data storage, memory devices etc [137]. The EB field (H_{EB}) and coercivity (H_C) of a system can be calculated by these formulas $H_{EB} = (H_L + H_R)/2$ and $H_C = (|H_L| + |H_R|)/2$, respectively, where H_L and H_R are the left and right coercive field [138].

Explanation of exchange-bias effect:

Fig.1.22 explains the EB phenomenology present in an FM/AFM structure. It is process can be understood in following five steps:

First: When the material is cooled below the ordering temperature (T_C) of the ferromagnetic system but above the Neel temperature (T_N) of antiferromagnetic system in the presence of a magnetic field ($T_N < T < T_C$), the exchange bias incepts in the FM/AFM material due to the interface coupling at the boundary of FM/AFM layers. Under the applied magnetic field, AFM spins are randomly orientated in a paramagnetic state, whereas the FM spins line are aligned in the direction of field.

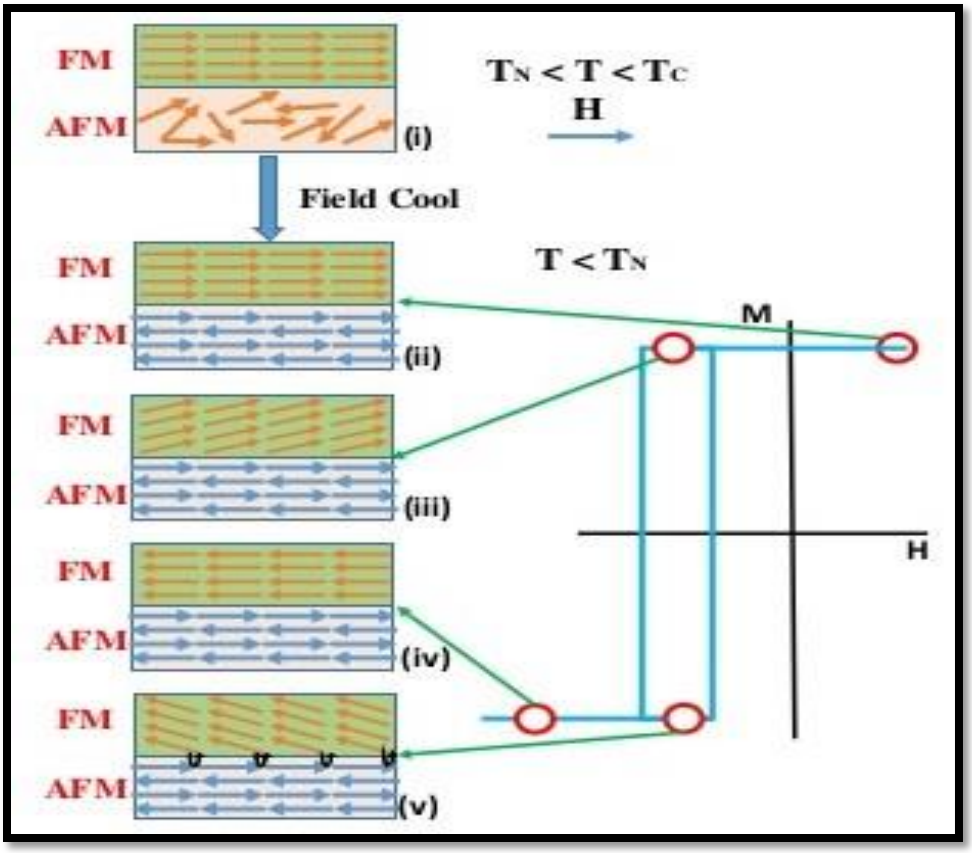

Figure 1.22: Shows the schematic explanation of exchange Bias effect.

Second: When the $T < T_N$, The first monolayer AFM spins are coupled with FM spins along the direction of field across the interface due to the exchange interaction. Another monolayer of AFM spins can follow the AFM nature i.e. coupled antiparallel to previous one, and it leads to a typical ferromagnetic hysteresis curve.

Third: A small finite magnetization originates at the monolayer due to the uncompensation of spins at the FM/AFM interface. During the reversal process of magnetization, FM and AFM both will stay in single domain state. When the magnetic field is being reversed, only FM spin has started to align along the direction of magnetic field as AFM spins remain in same state due to the strong AFM anisotropy at the FM/AFM interface.

Fourth: The extra reverse field is applied to align all FM spins along its direction. Moreover, FM spins become antiparallel to the AFM spins at the FM/AFM boundary. Therefore, the FM spin has unidirectional configuration.

Fifth: On applying a field in positive direction, the FM spins switches easily even at small magnetic field as they are coupled with AFM spins. Thus, the magnetic hysteresis curve is shifted towards the negative direction of the magnetic field from its center and the shifting of this hysteresis loop is known as exchange bias [139]. This type of obtained EB in presence of external magnetic field is known as conventional exchange bias (CEB). However, surprisingly, there is an observation of EB in absence of external magnetic field i.e. with no extra magnetic field, the system exhibit exchange bias. Such type of EB is known as spontaneous exchanger bias (SEB). In recent times systems with SEB gained have its own demand in research world due to its feature.

1.6.5 Magneto-dielectric coupling:

Magneto-dielectric coupling (MDC) leads to the process where an external magnetic field can alter the dielectric property of a system through internally coupled electrical and magnetic parameters [140, 141]. Generally, dielectric is the measurement of the degree of polarization in presence of an external electric field. Whereas, the magnetodielectric refers to the effect of magnetism on the dielectric properties of a material. Magneto-dielectric can be defined as

$$\text{MD } \% = \frac{\epsilon(\text{H}) - \epsilon(0)}{\epsilon(0)} \times 100 \tag{1.24}$$

where, $\epsilon(\text{H})$ is the value of dielectric constant at H magnetic field and $\epsilon(0)$ is the value of dielectric constant at zero magnetic field. The magneto-dielectric responses are an important

feature of multifunctional materials which are used in information storage and sensing applications [142, 143]. The asymmetric hopping on the spin orientations of neighboring sites in a material turns to magnetodielectric coupling in material.

1.6.6 Transport Property:

Double perovskite materials like La_2CoFeO_6, Pr_2CoFeO_6 show the semiconducting nature. Therefore, to understand the temperature dependent conductivity in such systems, thermally activated VRH model or Arrhenius model can be personated.

1.6.6.1Variable Range Hopping (VRH) Model:

The variable range hopping model is proposed by Sir Nevill Mott [144]. This model is used to determine the resistivity of disordered systems at low temperature. This law is stated as

$$\rho = \rho_o \exp(T_o/T)^{1/4} \tag{1.25}$$

where ρ_o is exponential factor and T_o is characteristic barrier energy temperature. VRH law is fitted on the lnρ versus $(1/T)^{0.25}$ curve as shown in fig. 1.23. This law also defines the electron hopping energy.

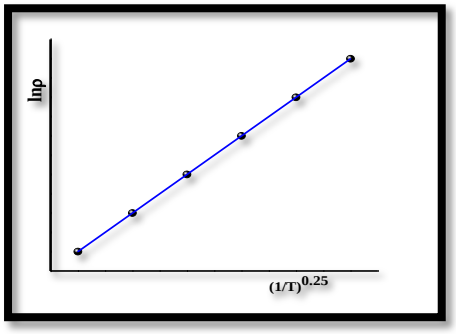

Figure 1.23: Shows the lnρ versus $(1/T)^{0.25}$ curve with VRH fit (blue colour).

1.6.6.2 Arrhenius law:

Dutch chemist, J.H van't Hoff has proposed the Arrhenius equation in 1884. However, Svante Arrhenius gave the physical interpretation of this Arrhenius equation. He used this equation for a chemical reaction to understand the dependency of the rate constant (k) on the activation energy (E_A) and temperature. For this purpose, the Arrhenius eq. is

$$k = A\exp(-E_A/RT) \tag{1.26}$$

where R is a gas constant. Generally, Arrhenius law is employed for thermally activated process. For electrical transport phenomenon, Arrhenius equation is stated as

$$\rho = \rho_o \exp(E_A/k_B T) \tag{1.27}$$

here, E_A is the activation energy and k_B is the Boltzman constant. This law is fitted on the lnρ vs. (1/T) curve as shown in fig. 1.24 (a).

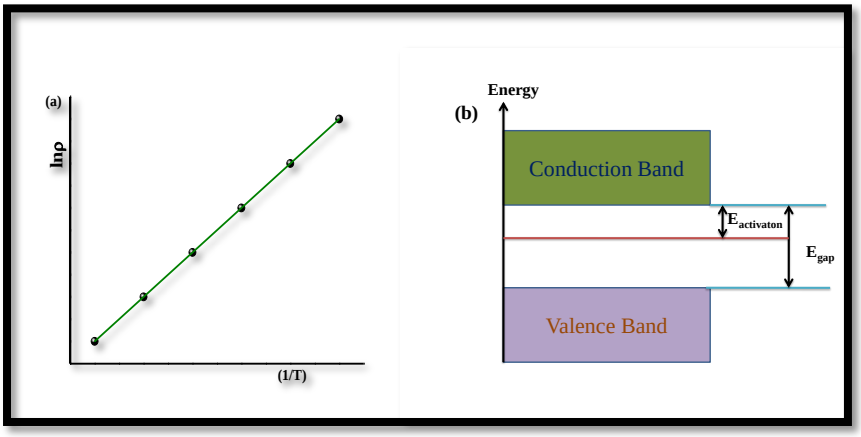

Figure 1.24: (a) Shows the lnρ versus (1/T) curve with Arrhenius fit (green colour). **(b)** Shows the activation energy and the band gap between valence and conduction bands.

1.7 Motivation of the thesis:

Geometrical spin frustration and disorder driven spin frustration both are one of the fascinating and promising subjects among the condensed matter research world. Existence of single ion spin freezing, wasp-waisted hysteresis loop, high temperature magnetic ordering,

exchange-bias, reentrant cluster glass state, magneto-dielectric like various properties place these systems at high note for investigation.

$Tb_2Ti_2O_7$ is one of the widely studied spin liquid compound, whereas $Eu_2Ti_2O_7$ pyrochlore is relatively less studied compound. Former studies on $Tb_2Ti_2O_7$ reported that it shows paramagnetic behaviour without any type of freezing at high temperature. Moreover, a magnetic field induced transition is observed at low temperature for this system due to single moment saturation [45]. On the other hand, $Eu_2Ti_2O_7$ system, a planar X-Y pyrochlore shows a single ion spin freezing at high temperature [67]. Thus, it is interesting to see the correlation of two different systems in which one system ($Tb_2Ti_2O_7$) is without spin freezing and one system ($Eu_2Ti_2O_7$) is with spin freezing at high temperature. The change in the crystal field levels of both Tb^{3+} and Eu^{3+} spins can alter the ground state of new pyrochlore. Thus, to explore the dynamic magnetic properties, we have investigated the $(Tb_{1-x}Eu_x)_2Ti_2O_7$ ($0 \leq x \leq 1.0$) by different measurement tools.

As mentioned earlier that $Eu_2Ti_2O_7$ exhibits a single ion spin freezing at high temperature. Whereas, $Dy_2Ti_2O_7$, a well-known and highly investigated spin ice compound shows two spin relaxation process at different temperature [55, 56]. As matter of fact, both systems shows single ion spin freezing i.e. $Dy_2Ti_2O_7$ exhibit high temperature spin freezing due to Dy^{3+} ions, while $Eu_2Ti_2O_7$ manifests high temperature spin relaxation due to Eu^{3+} ions. When the pyrochlore lattice possess both Eu^{3+} and Dy^{3+} spins at A-site, the crystal field scheme changes the behaviour of compound and it should show interesting magnetic properties. Hence, we have done extensive studied of $Dy_{2-x}Eu_xTi_2O_7$ ($0 \leq x \leq 2.0$) systems.

In case of disorder driven spin frustration, The Co/Ni/Mn based DP are widely studied. The studies on the Co/Fe based B-site disordered systems are particularly limited. So, there is

lot of possibilities to explore their properties. Moreover, Co and Fe ions have their own features as they have similar size and valance states in the periodic table. La based DP shows tremendous magnetic, electrical and transport property. The DP La_2CoFeO_6 undergoes a long range ordering at antiferromagnetic transition temperature (270 K) [68]. Whereas, another DP Pr_2CoFeO_6 has exhibited the Griffiths phase, spin glass, exchange bias and strong spin phonon coupling [70, 71]. Neutron diffraction study also revealed a G-type of AFM ordering occurs below 269 K. Thus, to see the lattice effect, we have substituted La ion by Pr ion in La_2CoFeO_6 DP. For this compound, both Co and Fe have similar oxidation sate (+3). We have investigated the multiple properties of $La_{1.8}Pr_{0.2}CoFeO_6$ compound.

It is already reported that the hole doping in manganite systems has originates the different properties in systems like giant exchange bias, colossal magneto-resistance etc. Moreover, hole doping creates the mixed valance states of B/B' ions. Therefore, to develop the interesting magnetic phenomenon like, exchange bias, double glassy nature etc in DP and existence of mixed valance states, we have prepared $La_{1.5}Ca_{0.5}CoFeO_6$. It is ravishing to study the effect of 3d transition Ca element on La site in La_2CoFeO_6 i.e. $La_{1.5}Ca_{0.5}CoFeO_6$ system.